

Synthesizing Physically Plausible Human Motions in 3D Scenes

Liang Pan¹, Jingbo Wang², Buzhen Huang¹, Junyu Zhang¹, Haofan Wang³, Xu Tang³, Yangang Wang¹

¹Southeast University ²Shanghai AI Lab ³Xiaohongshu Inc.

{liangpan, hbz, junyuzhang, yangangwang}@seu.edu.cn

wangjingbo@pjlab.org.cn, {wanghaofan, tangshen}@xiaohongshu.com

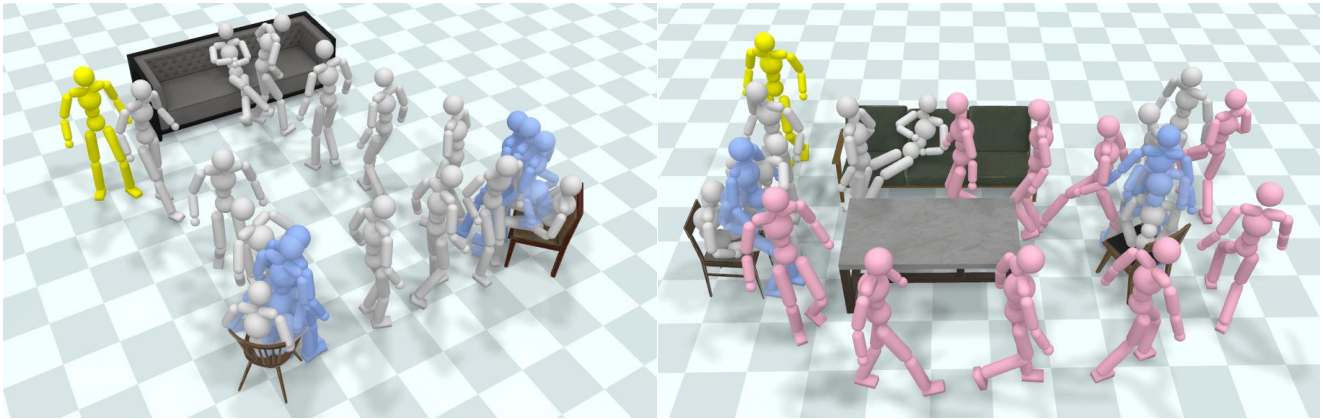


Figure 1. Our framework enables physically simulated characters to perform long-term interaction tasks in diverse and complex 3D scenes via composing reusable skills that include sitting (gray), getting up (blue), and avoiding obstacles (red).

Abstract

Synthesizing physically plausible human motions in 3D scenes is a challenging problem. Kinematics-based methods cannot avoid inherent artifacts (e.g., penetration and foot skating) due to the lack of physical constraints. Meanwhile, existing physics-based methods cannot generalize to multi-object scenarios since the policy trained with reinforcement learning has limited modeling capacity. In this work, we present a framework that enables physically simulated characters to perform long-term interaction tasks in diverse, cluttered, and unseen scenes. The key idea is to decompose human-scene interactions into two fundamental processes, **Interacting** and **Navigating**, which motivates us to construct two reusable **Controllers**, i.e., **InterCon** and **NavCon**. Specifically, **InterCon** contains two complementary policies that enable characters to enter and leave the interacting state (e.g., sitting on a chair and getting up). To generate interaction with objects at different places, we further design **NavCon**, a trajectory following policy, to keep characters' locomotion in the free space of 3D scenes. Benefiting from the divide and conquer strategy, we can train the policies in simple envi-

ronments and generalize to complex multi-object scenes. Experimental results demonstrate that our framework can synthesize physically plausible long-term human motions in complex 3D scenes. Code will be publicly released at <https://github.com/liangpan99/InterScene>.

1. Introduction

Creating virtual characters with diverse motor skills (e.g., walking, sitting, rising from seated positions) and rich human-scene interactions in daily living scenarios remains a fundamental undertaking within computer vision and graphics. While previous works [5, 9, 20, 27, 28, 31, 33] have achieved long-term motion generation for human-scene interactions, these models still suffer from physical artifacts, such as surface penetration and foot skating. Recent work [1, 6] began incorporating physics simulators to synthesize physically plausible motions. However, their frameworks remain constrained to interactions with single objects since the policy trained with reinforcement learning has limited modeling capacity and thus results in gaps between the generated motions and realistic human behaviors in complex 3D scenes.

To bridge the gaps, our work endeavors to enable physically simulated characters to perform long-term interaction tasks in cluttered multi-object environments. The key insight of our framework is to construct two reusable controllers, *i.e.*, **InterCon** and **NavCon**, for modeling two fundamental processes in human-scene interactions. InterCon learns skills of interacting with objects. NavCon controls characters’ movement along obstacle-free paths. The strengths lie in 1) our framework decomposes long-term interaction tasks into a scheduling problem of two controllers; 2) both controllers can be trained in relatively simple environments without relying on costly 3D scene data; 3) trained controllers can directly generalize to complex multi-object scenes without additional training.

Although existing works [1, 6] presented controllers for executing interaction tasks, they cannot be applied in multi-object scenarios due to incomplete interaction modeling. To address this issue, our InterCon employs two complementary control policies to learn complete interaction skills. Different from previous works [1, 6], InterCon not only involves reaching and interacting with the object but also includes leaving the interacting object. As illustrated in Fig 1 (left), leveraging the two policies guarantees InterCon is a closed loop controller, which realizes interactions with multiple objects. In cluttered environments with obstacles like Fig 1 (right), we further introduce NavCon to enable characters to navigate and avoid obstacles in complex multi-object scenarios. InterCon and NavCon provide complete interaction skills, including sitting, getting up, and obstacle-free trajectory following. Thus, we can leverage a finite state machine to schedule the two controllers, allowing characters to perform long-term interaction tasks in complex 3D scenes without additional training.

We train all policies by goal-conditioned reinforcement learning and adversarial motion priors (AMP) [17]. It is challenging to train InterCon stably because the policy needs to coordinate the character’s fine-grained movement in relation to the object, and the reward is sparse. Previous work [6] conditions the discriminator of AMP on the scene context to construct a dense reward. In this work, we propose interaction early termination to achieve stable training via balancing data distribution in training samples. To ensure that our InterCon can generalize to unseen objects, a large number of objects with diverse shapes is required for the training [6]. However, the get-up policy relies on various seated poses in plausible contact with objects (*e.g.*, without floating and penetration), which is difficult to obtain. To tackle this issue, we introduce seated pose sampling, where a trained sit policy will be used to generate plausible sitting poses without incurring additional costs of motion capture.

In summary, our main contributions are:

1. We propose a framework that enables physically simu-

lated characters to perform long-term interaction tasks in diverse, cluttered, and unseen 3D scenes.

2. We propose two reusable controllers for modeling interaction and navigation to decompose challenging human-scene interactions.
3. We leverage a finite state machine that enables users to obtain desired human-scene interactions through intuitive instructions without additional training.

2. Related Work

Human motion generation in 3D scenes. Creating virtual characters capable of interacting with surrounding environments is widely explored in computer vision and graphics. One of the streams of methods is to build data-driven kinematic models leveraging large-scale motion capture datasets [13]. Phase-based neural networks [7, 20–22] are widely used in generating natural and realistic human motions. Holden *et al.* [7] propose phase-functioned neural networks to produce motions where characters adapt to rough terrain. Strake *et al.* [20] extend the idea of phase variables to generate motions in human-scene interaction scenarios such as sitting on chairs and carrying boxes. Strake *et al.* [21] propose a local motion phase based model for synthesizing contact-rich interactions. An alternative approach uses generative models like conditional variance autoencoder (cVAE) to model human interaction behaviors. Wang *et al.* [27] present a hierarchical generative framework to synthesize long-term 3D motion conditioning on the 3D scene structure. Hassan *et al.* [5] present a stochastic scene-aware motion generation framework using two cVAE models for learning target goal position and human motion manifolds. Wang *et al.* [28] present a framework to synthesize diverse scene-aware human motions. Taheri *et al.* [24] and Wu *et al.* [29] design similar frameworks to generate whole-body interaction motions. Most recent works adopt reinforcement learning (RL) to develop control policies for motion generation. MotionVAE [10] is a most representative work that proposes a new paradigm for motion generation based on RL and generative models. Zhang *et al.* [32] extend MotionVAE to synthesize diverse digital humans in 3D scenes. Zhao *et al.* [33] present interaction policy and locomotion policies to synthesize human motions in 3D indoor scenes. Lee *et al.* [9] also use reinforcement learning and motion matching to solve the locomotion, action, and manipulation task in 3D scenes. In this work, we aim to synthesize 3D motions of interacting with everyday indoor objects (*e.g.*, chairs, sofas, and stools). Most relevant previous works are phase-based neural networks [20], cVAE-based generative models [5, 27, 28], and RL-based methods [9, 33].

Physics-based motion generation. Physics-based paradigm uses motion control and physics simula-

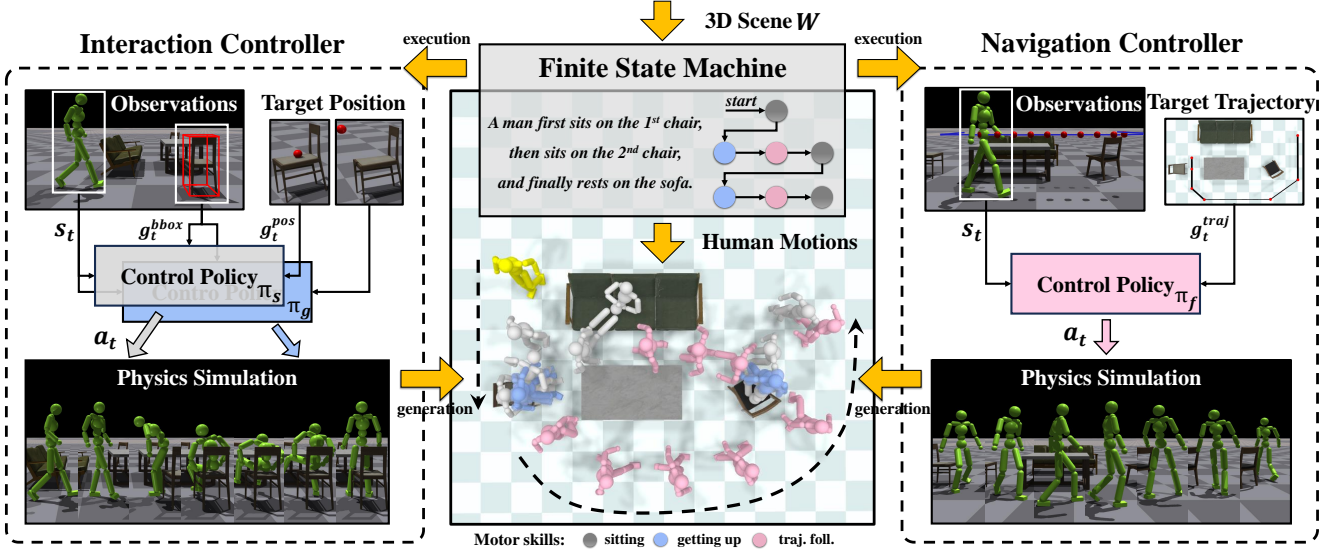


Figure 2. **Overview of our framework.** The interaction controller consists of two separate control policies, which provide two interaction-involved skills, *i.e.*, sitting and getting up. The navigation controller employs a trajectory following policy that controls the character’s movements along a specific path. Then, two reusable controllers are combined to synthesize human motions in complex 3D scenes without additional training. This is achieved by using a finite state machine that receives user instructions to enable the simulated character to perform long-term interaction tasks.

tors [14, 26] to guarantee the physical plausibility of the generated motions. Most efforts are devoted to improving the motion naturalness of physically simulated characters. Tracking-based motion imitation techniques [3, 11, 12, 16] enable simulated characters to imitate diverse, challenging, and natural motor skills. However, tracking-based methods rely on high-quality reference motions. It can be challenging to obtain such high-quality data in motion generation tasks. Recently, adversarial motion priors [17] present a generative motion imitation learning framework where a motion discriminator is trained to replace the complex tracking-based objectives. AMP-based works [8, 18, 25] have achieved impressive results in task-oriented motion generation. Recent work [6] first extends the AMP framework to synthesize character-scene interactions, such as sitting on chairs, lying on sofas, and carrying boxes. Similar tracking-based works [1, 30] also focus on character-scene interaction.

3. Method

3.1. Overview

As illustrated in Fig 2, our framework integrates two reusable controllers, *i.e.*, **Interaction Controller** (InterCon) and **Navigation Controller** (NavCon), serving as low-level executors, and a **Finite State Machine** (FSM), serving as a high-level planner to schedule the two executors to synthesize human motions according to user instructions. InterCon consists of two control policies, including sit policy π_s

and get-up policy π_g . Each policy is conditioned on the target object features g_t^{bbox} and the target position g_t^{pos} of the character’s root. NavCon contains a trajectory following policy π_f that is conditioned on the target trajectory features g_t^{traj} . These input conditions can be seen as explicit control signals.

We use the cluttered 3D scene W shown in Fig 2, which contains three interactable objects $W = \{w_1, w_2, w_3\}$, as an example to describe the workflow of our framework. Based on three control policies, our FSM provides users with three reusable skills, including sitting k_s , getting up k_g , and trajectory following k_f . To synthesize human motions described by “A man first sits on the 1st chair, then sits on the 2nd chair, and finally rests on the sofa”, the user needs to construct the following instruction:

$$I = \{(k_s, w_1), (k_g, w_1), (k_f, h_1), (k_s, w_2), (k_g, w_2), (k_f, h_2), (k_s, w_3)\}, \quad (1)$$

where $(k_s/k_g, w)$ denotes that the character performs the sitting skill k_s to sit on the object w or performs the getting up skill k_g to leave the object w , and (k_f, h) denotes that the character moves along an obstacle-free trajectory h that can be either generated by the A* path planning algorithm [4] or defined by the user. The FSM translates this instruction into a sequence of explicit control signals and then schedules control policies to execute the instruction without additional training. The FSM also determines when to tran-

sition between skills. For instance, the FSM will begin to execute the next skill when the overlapping time between the character’s root and its target position is greater than a specific time. Introducing such a simple rule-based FSM allows users to obtain desired long-term human motions in complex 3D scenes.

3.2. Reinforcement Learning Background

We formulate motion synthesis with goal-conditioned reinforcement learning. At each time step t , the policy $\pi(a_t|s_t, g_t)$ outputs an action a_t based on the current state s_t observed from the environment and the task-specific goal features g_t . Applied that action to the character, the environment transitions to the next state s_{t+1} based on the dynamics of the environment $p(s_{t+1}|s_t, a_t)$. A trajectory of simulated states describes a sequence of generated human poses, represented as $S = \{s_0, \dots, s_{t-1}, s_t\}$. The state s describes the configuration of the character’s body with 125D features including:

- Root height (1D)
- Root rotation (6D)
- Root linear and angular velocity (6D)
- Local joints rotations (72D)
- Local joints velocities (28D)
- Key joints positions: hands and feet (12D)

The root height is recorded in the world coordinate frame, and others are computed in the character’s local coordinate frame. Rotations are presented using a 6D representation [34]. The simulated character is the same as [6, 17, 18] that has 12 movable internal joints with a total of 28 degrees of freedom. The action $a \in \mathbb{R}^{28}$ from the policy specifies target orientations for PD controllers at each joint.

Our framework consists of three control policies, *i.e.*, sit policy π_s , get-up policy π_g , and trajectory following policy π_f . To train them to control physically simulated characters in a natural and life-like manner, we use the Adversarial Motion Priors (AMP) framework [17]. AMP enables characters to compose disparate skills depicted in large unstructured motion datasets to perform tasks. The policy π is trained to maximize the expected discounted return $J(\pi)$, where the reward r is formulated as:

$$r = w^G r^G + w^S r^S. \quad (2)$$

The task reward r^G encourages the character to accomplish desired tasks. The style reward r^S encourages the character to produce behaviors similar to datasets, which is computed by a discriminator $D(s_{t-10:t})$ based on 10 consecutive steps of state. More details can be found in [17]. Our framework involves three task scenarios, *i.e.*, sitting on chairs, getting up from seated positions, and following trajectories. In the subsequent sections, we will describe each task scenario’s goal features g and task reward function r^G .

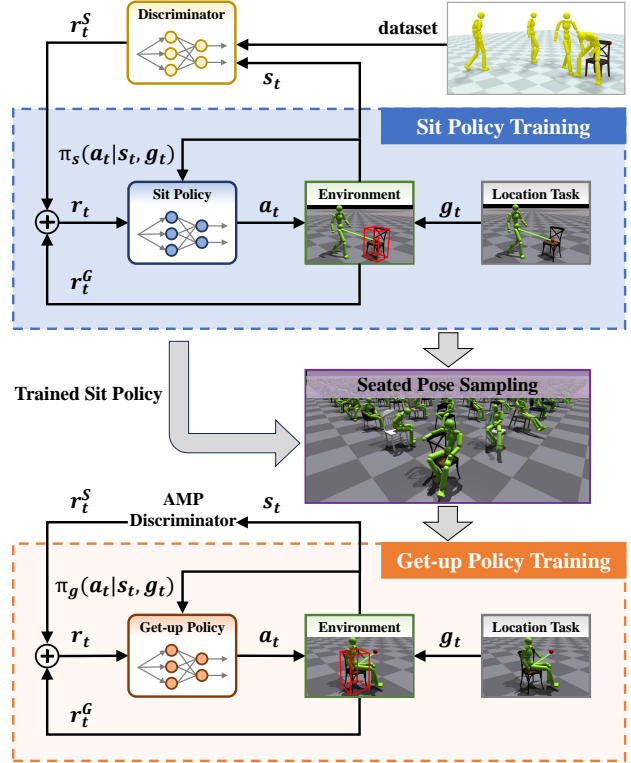


Figure 3. **The training scheme of the two control policies in InterCon.** It consists of three steps: 1) we first train an effective sit policy using the adversarial motion priors framework; 2) Due to the lack of high-quality seated pose data, we introduce the seated pose sampling, where a trained sit policy is employed to generate various poses; 3) finally, we begin training the get-up policy. The initialization leverages synthetic seated poses to initialize the character at the beginning of the episode.

3.3. Interaction Controller

Given a target object $w_i \in W$, InterCon enables a character to enter or leave the interacting state with the object. Previous physics-based methods [1, 6] mainly focus on developing the former ability for the character, overlooking the importance of the latter for long-term interaction tasks. By learning the skill of getting up, InterCon can recover a seated character to stand still, which provides the opportunity to continue performing new interaction tasks.

As illustrated in Fig. 2, InterCon consists of two separate control policies, *i.e.*, sit policy π_s and get-up policy π_g . Each policy shares the same state s_t , goal features $g_t = \{g_t^{bbox}, g_t^{pos}\}$, and network structure. To make the policy aware of the target object, we condition the policy on the target object’s 3D features $g_t^{bbox} \in \mathbb{R}^{24+2}$ that contain 8 vertices of the bounding box and a horizontal vector of the facing direction. This is crucial for policy to effectively learn how to coordinate a character’s movements in relation

to the target object. In particular, we add explicit target position g_t^{pos} of the character’s root into the goal features g_t . The target position of the sit policy is placed 5cm above the center of the chair seat’s top surface, and the target position of the get-up policy is computed by:

$$g_t^{pos} = \left[\frac{j_{l_foot}^x + j_{r_foot}^x}{2}, \frac{j_{l_foot}^y + j_{r_foot}^y}{2}, 0.89 \right] \quad (3)$$

where j_i represents 3D position of i joint, we use steady sitting poses to compute g_t^{pos} of the get-up policy. All these goal features are recorded in the character’s local frame.

Training. Our training scheme of two control policies is illustrated in Fig 3. While the proposed InterCon is applied in complex multi-object environments, we train the policies in relatively simple single-object environments without the reliance on costly 3D scene data. Similar to [6], we follow the standard AMP framework and extend it to character-scene interaction tasks to train each policy in InterCon. We first describe the training procedures for the sit policy.

- **Motion and object datasets.** We use 20 sequences from the SAMP dataset [5] (*chair_mo001* ~ *chair_mo019*). Since the SAMP dataset provides motions represented by SMPL-X [15] parameters, we retarget motions to our simulated character. To ensure that trained policy can generalize well to new objects, we follow [6] to select 57 chairs with diverse shapes and scales in the 3D-Front dataset [2] and randomly divide 50 as the training set and 7 as the testing set.
- **Initialization.** At the start of each episode, objects are randomly sampled from the training set and initialized to fixed positions and rotations recorded by the SAMP dataset. For the character, we initialize it using two methods. The one is reference state initialization [16]. The other is placing a character with a default pose and a random global rotation sampled uniformly between $[0, 2\pi]$ anywhere between one and five meters away from the object’s 2D center.
- **Reward.** The total reward is defined in Eq 2. The style reward is modeled using a motion discriminator. Unlike [6], we do not condition the discriminator on the object context. Given a target position of character’s root g_t^{pos} and a target scalar velocity g_t^{vel} , the task reward is defined as:

$$r_t^G = \begin{cases} 0.7 r_t^{near} + 0.3 r_t^{far}, & \|x^* - x_t^{root}\|^2 > 0.5 \\ 0.7 r_t^{near} + 0.3, & \text{otherwise} \end{cases} \quad (4)$$

$$\begin{aligned} r_t^{far} = & 0.5 \exp(-0.5 \|x^* - x_t^{root}\|^2) \\ & + 0.4 \exp(-2.0 \|g_t^{vel} - d_t^* \cdot \dot{x}_t^{root}\|^2) \\ & + 0.1 \|d_t^* \cdot d_t^{facing}\|^2 \end{aligned} \quad (5)$$

$$r_t^{near} = \exp(-10.0 \|g_t^{pos} - x_t^{root}\|^2) \quad (6)$$

where x_t^{root} is the 3D position of the character’s root, x^* is the 3D position of the object center, d^* is a horizontal unit vector pointing from x_t^{root} to x^* , d_t^{facing} is a horizontal unit vector of character’s facing direction, $a \cdot b$ represents vector dot product.

- **Reset and early termination conditions.** An episode terminates after a fixed episode length or when early termination (ET) conditions have been triggered. The episode length is set to 10 seconds. We use fall detection as one of ET’s conditions. We introduce a new condition called interaction early termination (IET). IET terminates an episode when the accumulative overlapping time between the character’s root X_t^{root} and the target position g_t^{pos} has exceeded a fixed period of time. Experimental results show that the simple IET mechanism can effectively stabilize RL training.

Training the get-up policy. As shown in Fig 3, we begin training the get-up policy after the sit policy is trained. We keep most of the settings described above except for the initialization part. To initialize the character at the beginning of each episode, we rely on diverse seated poses in plausible contact with objects, with no floating or penetration. Such high-quality data is difficult to obtain due to the large number of objects in the training set. Thus, we use a trained sit policy to sample a lot of physically plausible sitting poses. This is the key to train the get-up policy successfully.

3.4. Navigation Controller

While InterCon can synthesize long-term interaction motions, it cannot avoid obstacles in cluttered 3D scenes. To present a simulated character capable of performing obstacle-free locomotion, we propose NavCon, which contains a trajectory following policy $\pi_f(a_t|s_t, g_t^{traj})$, as shown in Fig 2. We follow [19] to construct the goal features by a short trajectory $g_t^{traj} \in \mathbb{R}^{10 \times 2}$ consisting of a series of 2D positions of the character’s root for the next 2.5 seconds sampled at 0.25s intervals. Incorporating a module for acquiring collision-free human locomotion has been widely adopted by previous works [5, 28, 33]. However, kinematics-based methods produce foot skating artifacts. Physics-based trajectory following [19] can generate physically plausible locomotion of characters. In this work, we first apply this technique to character-scene interaction tasks. Using NavCon makes our framework a closed-loop framework for synthesizing long-term human motions in human-scene interaction scenarios and provides an interface for users to generate human-scene interactions with the custom locomotion trajectories.

Training. We train the trajectory following policy according to the settings given by [19]. In our case, the policy is

Method	Success Rate (%)	Execution Time (s)	Precision (m)
NSM	75.0	7.5	0.19
SAMP	75.0	7.2	0.06
Chao <i>et al.</i>	17.0	–	–
InterPhys	93.7	3.7	0.09
AMP	56.6	7.5	0.06
Ours	97.8	2.6	0.04

Table 1. Comparisons on the sitting task with kinematics-based methods, *i.e.*, NSM [20], SAMP [5] and physics-based methods, *i.e.*, Chao *et al.* [1], InterPhys [6], AMP [17]. We report metrics including success rate, execution time, and precision. All metrics are averaged over 4096 trials.

Epoch (1e3)	Success Rate (%)	Execution Time (s)	Precision (m)
5	87.9	0.8	0.08
8	91.7	0.4	0.05
12	93.5	0.3	0.08

Table 2. Quantitative results of the get-up policy.

IET (steps)	Success Rate (%)	Execution Time (s)	Precision (m)
–	56.6	7.5	0.06
120	60.4	6.3	0.04
90	79.1	5.9	0.05
60	85.0	4.8	0.04
30	97.8	2.6	0.04

Table 3. Quantitative results of the sit policy trained with different step parameters of the interaction early termination mechanism (IET).

trained in simple environments with flat ground, unlike [19] that uses complex terrains.

- **Motion and trajectory datasets.** We use ~ 200 sequences from the AMASS dataset [13]. We also retarget motion sequences to our used character. We follow [19] to procedurally generate synthetic trajectories for training. A complete trajectory $\tau = \{p_0^\tau, \dots, p_{T-1}^\tau, p_T^\tau\}$ is modeled as a set of 2D points with a fixed 0.1 seconds time interval. At each time step t , we query 10 points $\{p_t^\tau, \dots, p_{t+9}^\tau\}$ in the future 2.5 seconds from the complete trajectory τ by interpolating to construct the goal features g_t^{traj} .
- **Other settings.** We terminate the training episode when the character is fallen or deviates too far from the established trajectory. Characters are always initialized to a fixed default state. Trajectories will be re-computed when environments reset. The task reward r_t^G measures how far away the character’s root x_t^{root} on the horizontal plane from the desired location $p_t^\tau \in \tau$, formulated as:

$$r_t^G = \exp(-2.0 \|x_t^{root} - p_t^\tau\|^2). \quad (7)$$

4. Experiment

4.1. Evaluation on Interaction Controller

InterCon consists of two control policies responsible for

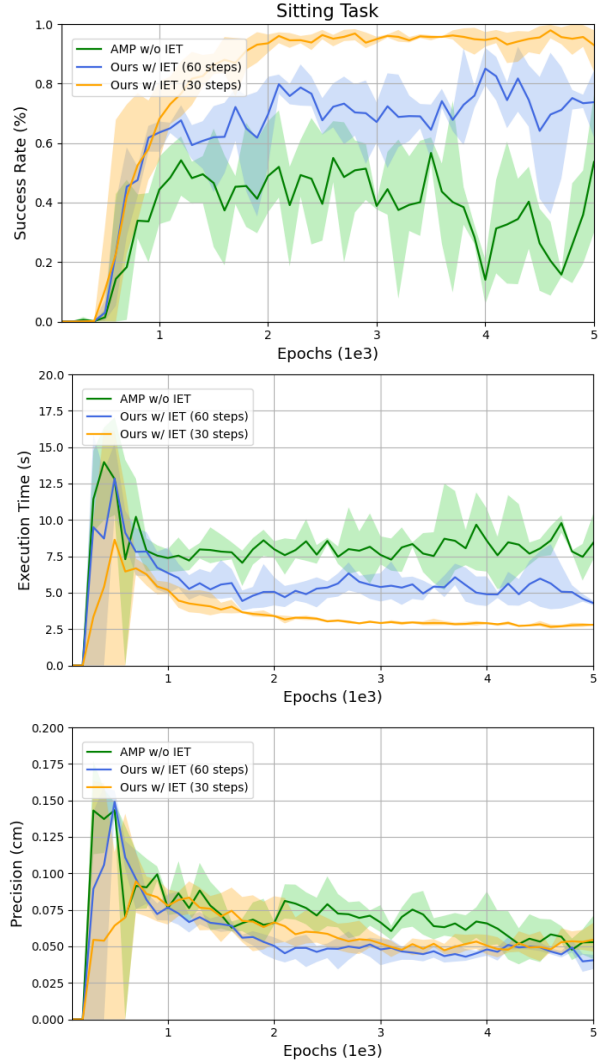


Figure 4. Performance curves of the sit policy trained with different step parameters of the interaction early termination mechanism (IET).

performing the sitting and getting up tasks. We first quantitatively evaluate the effectiveness of each policy in its corresponding task. Then, we conduct ablation studies on the hyperparameter of interaction early termination (IET). We evaluate the model performance by measuring the success rate, which indicates the percentage of trials where the character accomplishes the task. A trial will be determined to be successful if the Euclidean distance between the character’s root and the goal position is less than 20 cm. We further evaluate the quality of successful trials using: 1) execution time, the average time the character spends to complete the task; 2) precision, the average distance between the character’s root and its goal position. All metrics are computed over 4096 trials per task.

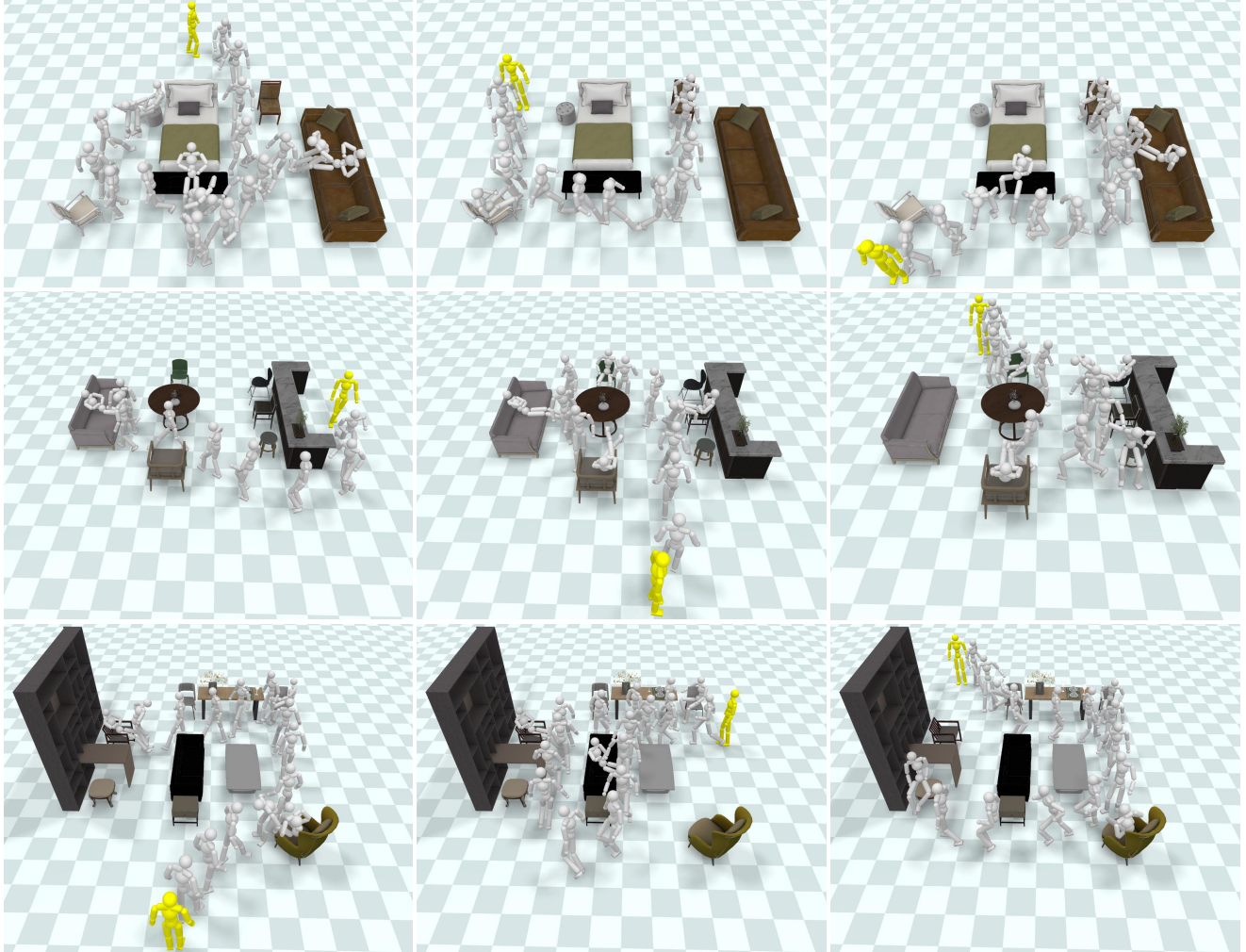


Figure 5. Long-term human motions in three complex 3D scenes generated by our complete system.

3D scenes. In this section, we conduct experiments on single-object environments. We use 7 unseen chairs from the 3D-Front dataset [2]. We initialize the environment for each trial with an object randomly sampled from the dataset.

The effectiveness of the sit policy. We evaluate the effectiveness in the sitting task. The character is randomly initialized anywhere between 1 m and 5 m away from the object and with a random orientation. The maximum episode length is set to 20 seconds. We adopt AMP [17] as the baseline, where all training configurations (*e.g.*, state, action, reward, dataset) are the same as our method, except for the early termination conditions. The AMP baseline terminates the episode if the character has fallen. We train our sit policy using an additional condition, *i.e.*, interaction early termination, where the maximum interaction step is set to 40 steps. Table 1 shows the empirical evaluation results. We report the numbers provided in [6] of NSM [20], SAMP [5],

Chao *et al.* [1], and InterPhys [6]. We train our method and the baseline three times with different random seeds and report the best averaged metrics. Our sit policy achieves a high success rate and significantly exceeds the baseline, which demonstrates the effectiveness of our sit policy.

The effectiveness of the get-up policy. We evaluate the effectiveness in the getting up task. We first use a trained sit policy to generate various seated poses on the 7 testing objects. Because the character can sit on the chair facing three different directions, we collect 30 samples in each direction, resulting in a total of $7 \times 3 \times 30$ poses. The character is randomly initialized to a seated position sampled from 30 poses corresponding to the object. According to Table 2, our get-up policy can achieve a high success rate in the getting up task.

Ablation studies on IET. We train the sit policy multiple times with different step parameters of interaction early ter-

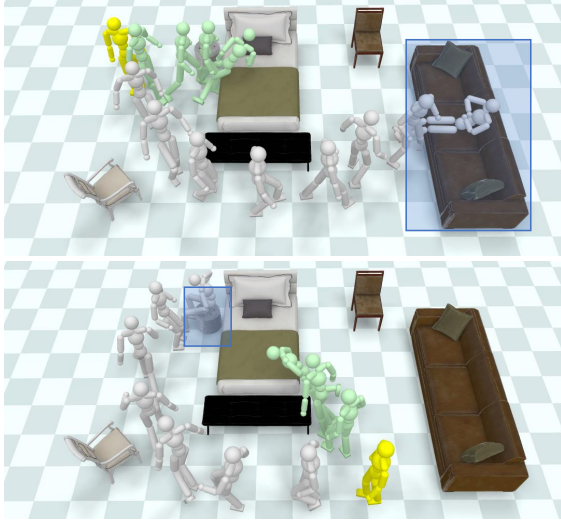


Figure 6. Comparisons on generated results between our complete system (gray) and a variant without NavCon (green). The blue rectangle denotes the target object.

mination. We also train each experiment three times to mitigate randomness. Table 3 shows the quantitative results, which indicate that the model performance gradually improves as the number of steps decreases. As shown in Fig 4, using a smaller step parameter can significantly reduce the fluctuation of the performance curve and achieve better convergence and stability, which demonstrates our novel interaction early termination can effectively stabilize the training process of InterCon.

4.2. Evaluation on Complete System

Although each controller is trained in single-object or no-object environments, incorporating them enables our complete system to successfully synthesize long-term human motions in diverse and complex 3D scenes without additional training. To demonstrate the effectiveness of our system, we apply it in three testing 3D scenes. For each scene, we manually design three scripts, each containing a series of interaction tasks for the character to perform. The finite state machine will schedule the two controllers according to the script.

3D scenes. We construct three synthetic scenes to simulate everyday indoor scenes. 3D Object meshes come from the 3D-Front dataset [2]. Unlike the experiment in 4.1, we use a wider variety of objects, some even out-of-distribution. We use 17 objects (6 straight chairs, 4 armchairs, 3 sofas, 4 stools). Each scene is populated with 5 ~ 6 interactable objects and some obstacles.

Results. As shown in Fig 5, our complete system can successfully synthesize desired long-term human-scene inter-

action motions. Results demonstrate that our method can be generalize to diverse, cluttered, and completely unseen 3D scenes. We also validate that InterCon can generalize its learned interaction skills to new objects, even for out-of-distribution objects like sofas. And the ability to avoid obstacles provided by NavCon effectively helps the simulated character interact with multiple objects in different places.

4.3. Ablation on Navigation Controller

Our system relies on NavCon to ensure characters can navigate in cluttered environments while avoiding obstacles. We validate its importance by comparing results produced by our complete system and a variant without NavCon. As shown in Fig 6, given the same target, the complete system first uses NavCon to prompt the character to approach the object by tracking an obstacle-free path and then uses InterCon to control the character to successfully interact with the object. However, the variant can only exploit InterCon, which always tends to follow the shortest path to the target object, causing the character to get stuck by obstacles. Therefore, introducing NavCon into our system is critical for synthesizing motions in complex environments.

5. Limitations and Future Work

InterCon’s purpose is to learn interaction-involved skills. Our trained InterCon focuses on sitting behavior. However, human-scene interactions also contain other behaviors, such as lying and touching. Current research does not include these actions. Since InterCon is a plug-and-play module, we can accommodate more actions into our framework by adding new interaction controllers trained for each action. According to previous work [6], training separate controllers for each action is practical. The trajectory following policy of NavCon tracks a pre-planned obstacle-free path. However, the character can still possibly get stuck by obstacles due to tracking errors, interrupting the established path. We will incorporate a dynamic path planning algorithm [23] to address this problem in future work. We model virtual characters with a fixed skeletal humanoid. We will use skinned human body models for more realistic surface contact in future work.

6. Conclusion

In this paper, we present a physics-based framework to synthesize long-term human-scene interaction motions. This is achieved by jointly using two reusable controllers, *i.e.*, InterCon and NavCon, to simplify the long-term motion generation task. Our physically simulated characters realistically and naturally present interaction and locomotion behaviors in diverse, cluttered, and unseen 3D scenes.

References

- [1] Yu-Wei Chao, Jimei Yang, Weifeng Chen, and Jia Deng. Learning to sit: Synthesizing human-chair interactions via hierarchical control. In *Proceedings of the AAAI Conference on Artificial Intelligence*, pages 5887–5895, 2021. 1, 2, 3, 4, 6, 7
- [2] Huan Fu, Bowen Cai, Lin Gao, Ling-Xiao Zhang, Jiaming Wang, Cao Li, Qixun Zeng, Chengyue Sun, Rongfei Jia, Binqiang Zhao, et al. 3d-front: 3d furnished rooms with layouts and semantics. In *Proceedings of the IEEE/CVF International Conference on Computer Vision*, pages 10933–10942, 2021. 5, 7, 8, 1
- [3] Levi Fussell, Kevin Bergamin, and Daniel Holden. Super-track: Motion tracking for physically simulated characters using supervised learning. *ACM Transactions on Graphics (TOG)*, 40(6):1–13, 2021. 3
- [4] Peter E Hart, Nils J Nilsson, and Bertram Raphael. A formal basis for the heuristic determination of minimum cost paths. *IEEE transactions on Systems Science and Cybernetics*, 4(2):100–107, 1968. 3
- [5] Mohamed Hassan, Duygu Ceylan, Ruben Villegas, Jun Saito, Jimei Yang, Yi Zhou, and Michael J Black. Stochastic scene-aware motion prediction. In *Proceedings of the IEEE/CVF International Conference on Computer Vision*, pages 11374–11384, 2021. 1, 2, 5, 6, 7
- [6] Mohamed Hassan, Yunrong Guo, Tingwu Wang, Michael Black, Sanja Fidler, and Xue Bin Peng. Synthesizing physical character-scene interactions. *arXiv preprint arXiv:2302.00883*, 2023. 1, 2, 3, 4, 5, 6, 7, 8
- [7] Daniel Holden, Taku Komura, and Jun Saito. Phase-functioned neural networks for character control. *ACM Transactions on Graphics (TOG)*, 36(4):1–13, 2017. 2
- [8] Jordan Juravsky, Yunrong Guo, Sanja Fidler, and Xue Bin Peng. Padl: Language-directed physics-based character control. In *SIGGRAPH Asia 2022 Conference Papers*, pages 1–9, 2022. 3
- [9] Jiye Lee and Hanbyul Joo. Locomotion-action-manipulation: Synthesizing human-scene interactions in complex 3d environments. *arXiv preprint arXiv:2301.02667*, 2023. 1, 2
- [10] Hung Yu Ling, Fabio Zinno, George Cheng, and Michiel Van De Panne. Character controllers using motion vaes. *ACM Transactions on Graphics (TOG)*, 39(4):40–1, 2020. 2
- [11] Libin Liu, KangKang Yin, Michiel Van de Panne, Tianjia Shao, and Weiwei Xu. Sampling-based contact-rich motion control. In *ACM SIGGRAPH 2010 papers*, pages 1–10, 2010. 3
- [12] Libin Liu, KangKang Yin, and Baining Guo. Improving sampling-based motion control. In *Computer Graphics Forum*, pages 415–423. Wiley Online Library, 2015. 3
- [13] Naureen Mahmood, Nima Ghorbani, Nikolaus F Troje, Gerard Pons-Moll, and Michael J Black. Amass: Archive of motion capture as surface shapes. In *Proceedings of the IEEE/CVF international conference on computer vision*, pages 5442–5451, 2019. 2, 6
- [14] Viktor Makovychuk, Lukasz Wawrzyniak, Yunrong Guo, Michelle Lu, Kier Storey, Miles Macklin, David Hoeller, Nikita Rudin, Arthur Allshire, Ankur Handa, et al. Isaac gym: High performance gpu-based physics simulation for robot learning. *arXiv preprint arXiv:2108.10470*, 2021. 3, 1
- [15] Georgios Pavlakos, Vasileios Choutas, Nima Ghorbani, Timo Bolkart, Ahmed AA Osman, Dimitrios Tzionas, and Michael J Black. Expressive body capture: 3d hands, face, and body from a single image. In *Proceedings of the IEEE/CVF conference on computer vision and pattern recognition*, pages 10975–10985, 2019. 5
- [16] Xue Bin Peng, Pieter Abbeel, Sergey Levine, and Michiel Van de Panne. Deepmimic: Example-guided deep reinforcement learning of physics-based character skills. *ACM Transactions On Graphics (TOG)*, 37(4):1–14, 2018. 3, 5
- [17] Xue Bin Peng, Ze Ma, Pieter Abbeel, Sergey Levine, and Angjoo Kanazawa. Amp: Adversarial motion priors for stylized physics-based character control. *ACM Transactions on Graphics (ToG)*, 40(4):1–20, 2021. 2, 3, 4, 6, 7
- [18] Xue Bin Peng, Yunrong Guo, Lina Halper, Sergey Levine, and Sanja Fidler. Ase: Large-scale reusable adversarial skill embeddings for physically simulated characters. *ACM Transactions On Graphics (TOG)*, 41(4):1–17, 2022. 3, 4
- [19] Davis Rempe, Zhengyi Luo, Xue Bin Peng, Ye Yuan, Kris Kitani, Karsten Kreis, Sanja Fidler, and Or Litany. Trace and pace: Controllable pedestrian animation via guided trajectory diffusion. In *Proceedings of the IEEE/CVF Conference on Computer Vision and Pattern Recognition*, pages 13756–13766, 2023. 5, 6
- [20] Sebastian Starke, He Zhang, Taku Komura, and Jun Saito. Neural state machine for character-scene interactions. *ACM Trans. Graph.*, 38(6):209–1, 2019. 1, 2, 6, 7
- [21] Sebastian Starke, Yiwei Zhao, Taku Komura, and Kazi Zaman. Local motion phases for learning multi-contact character movements. *ACM Transactions on Graphics (TOG)*, 39(4):54–1, 2020. 2
- [22] Sebastian Starke, Ian Mason, and Taku Komura. Deepphase: Periodic autoencoders for learning motion phase manifolds. *ACM Transactions on Graphics (TOG)*, 41(4):1–13, 2022. 2
- [23] Anthony Stentz. Optimal and efficient path planning for partially-known environments. In *Proceedings of the 1994 IEEE international conference on robotics and automation*, pages 3310–3317. IEEE, 1994. 8
- [24] Omid Taheri, Vasileios Choutas, Michael J Black, and Dimitrios Tzionas. Goal: Generating 4d whole-body motion for hand-object grasping. In *Proceedings of the IEEE/CVF Conference on Computer Vision and Pattern Recognition*, pages 13263–13273, 2022. 2
- [25] Chen Tessler, Yoni Kasten, Yunrong Guo, Shie Mannor, Gal Chechik, and Xue Bin Peng. Calm: Conditional adversarial latent models for directable virtual characters. In *ACM SIGGRAPH 2023 Conference Proceedings*, pages 1–9, 2023. 3
- [26] Emanuel Todorov, Tom Erez, and Yuval Tassa. Mujoco: A physics engine for model-based control. In *2012 IEEE/RSJ international conference on intelligent robots and systems*, pages 5026–5033. IEEE, 2012. 3
- [27] Jiashun Wang, Huazhe Xu, Jingwei Xu, Sifei Liu, and Xiaolong Wang. Synthesizing long-term 3d human motion and interaction in 3d scenes. In *Proceedings of the IEEE/CVF Con-*

- ference on Computer Vision and Pattern Recognition*, pages 9401–9411, 2021. [1](#), [2](#)
- [28] Jingbo Wang, Yu Rong, Jingyuan Liu, Sijie Yan, Dahua Lin, and Bo Dai. Towards diverse and natural scene-aware 3d human motion synthesis. In *Proceedings of the IEEE/CVF Conference on Computer Vision and Pattern Recognition*, pages 20460–20469, 2022. [1](#), [2](#), [5](#)
- [29] Yan Wu, Jiahao Wang, Yan Zhang, Siwei Zhang, Otmar Hilliges, Fisher Yu, and Siyu Tang. Saga: Stochastic whole-body grasping with contact. In *European Conference on Computer Vision*, pages 257–274. Springer, 2022. [2](#)
- [30] Zhaoming Xie, Jonathan Tseng, Sebastian Starke, Michiel van de Panne, and C Karen Liu. Hierarchical planning and control for box loco-manipulation. *arXiv preprint arXiv:2306.09532*, 2023. [3](#)
- [31] Xiaohan Zhang, Bharat Lal Bhatnagar, Sebastian Starke, Vladimir Guzov, and Gerard Pons-Moll. Couch: Towards controllable human-chair interactions. In *European Conference on Computer Vision*, pages 518–535. Springer, 2022. [1](#)
- [32] Yan Zhang and Siyu Tang. The wanderings of odysseus in 3d scenes. In *Proceedings of the IEEE/CVF Conference on Computer Vision and Pattern Recognition*, pages 20481–20491, 2022. [2](#)
- [33] Kaifeng Zhao, Yan Zhang, Shaofei Wang, Thabo Beeler, and Siyu Tang. Synthesizing diverse human motions in 3d indoor scenes. *arXiv preprint arXiv:2305.12411*, 2023. [1](#), [2](#), [5](#)
- [34] Yi Zhou, Connelly Barnes, Jingwan Lu, Jimei Yang, and Hao Li. On the continuity of rotation representations in neural networks. In *Proceedings of the IEEE/CVF Conference on Computer Vision and Pattern Recognition*, pages 5745–5753, 2019. [4](#)

Synthesizing Physically Plausible Human Motions in 3D Scenes

Supplementary Material

Sec 7 demonstrates the scalability of our method by introducing a new action into our framework. Sec 8 describes implementation details. Video results are included in the supplementary video. Testing code and required data are provided. We highly encourage readers to view them to better understand our framework’s capabilities.

7. Learning to Lie Down

We introduce a new action, lying down, into our framework by training an additional interaction controller that specifically learns to lie down and get up. It can be added into our framework as a new low-level executor, providing more skills for the finite state machine.

Training. The training process of two control policies in interaction controller is highly similar to Sec 3.3. We briefly describe the difference.

- **Motion and object datasets.** We use 31 sequences from the SAMP dataset [5] and 57 sofas in the 3D-Front dataset [2] and randomly divide 50 as the training set and 7 as the testing set.
- **Initialization.** We use a hybrid of reference state and default state initialization to initialize the character at the beginning of each episode. To avoid penetration, the character is placed anywhere between two and five meters away from the object’s 2D center in the default state initialization mode.
- **Reward for training lie policy.** The task reward r_t^G and r_t^{far} are the same as Eq. 4. r_t^{near} is defined as:

$$\exp(-10.0(\|g_t^{pos} - x_t^{root}\|^2 + \|g_t^h - x_t^{head}\|^2)) \quad (8)$$

where x_t^{head} is the height of the character’s head, g_t^h is the target height.

- **Reward for training get-up policy.** The task reward r_t^G is defined as:

$$\begin{aligned} r_t^G = & 0.5 \exp(-10.0 \|g_t^{pos} - x_t^{root}\|^2) \\ & + 0.3 \exp(-10.0 \|g_t^h - x_t^{feet}\|^2) \\ & + 0.2 \exp(-10.0 \|g_t^h - x_t^{head}\|^2) \end{aligned} \quad (9)$$

where x_t^{feet} is the mean height of the character’s feet.

Results. As shown in Fig 7, the additional “lie down” interaction controller enables characters to lie down and get up

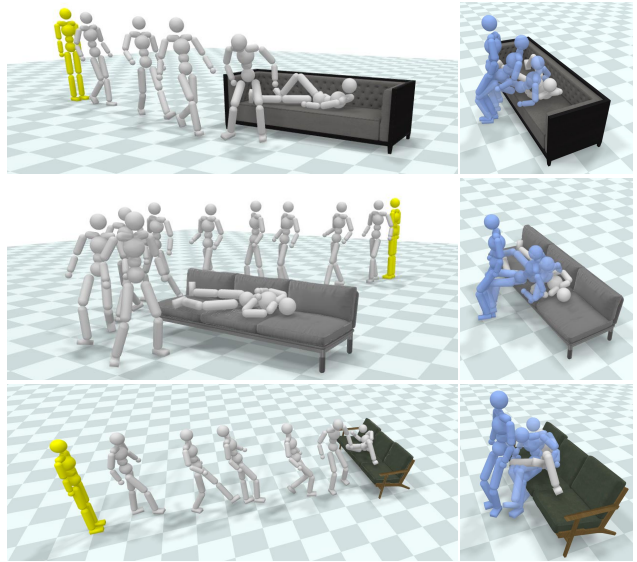


Figure 7. Synthesized results of the “lie down” interaction controller in single-object environments.

Parameter	Value
number of environments	6144
batch size for PPO	16384
batch size for AMP	4096
horizon length	32
learning rate	5e-5
clip range ϵ for PPO	0.2
discount factor γ	0.99
GAE coefficient λ	0.95

Table 4. Values of hyperparameters for training.

from unseen sofas successfully. Leveraging two separate interaction controllers, our extended framework enable physically simulated characters to interact with objects more diversely, as illustrated in Fig 8 and supplementary video.

8. Implementation Details

Physics simulation. We adopt NVIDIA’s GPU-based simulator, Isaac Gym [14]. The simulation runs at 60Hz while the policy controls the character at 30Hz.

Policy training. The policy uses a two layer MLP with hidden dimensions (1024, 512) and ReLU activations. The value of diagonal covariance matrix is set to 0.055. Proximal policy optimization (PPO) is used to train the policy. Hyperparameters are described in Table 4. Training each policy takes ~ 12 hours on one NVIDIA Tesla V100.

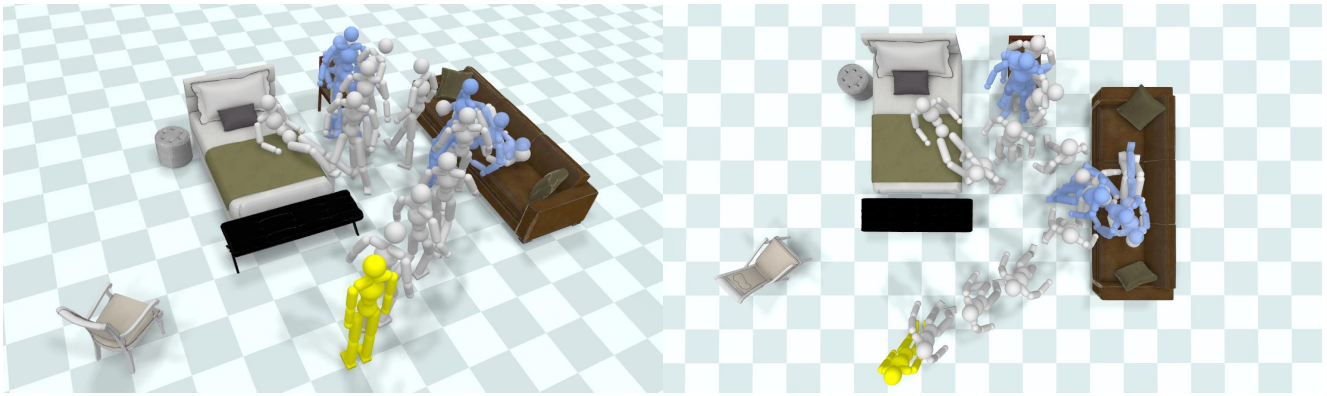


Figure 8. Synthesized results of our extended framework. The character first lies down on the sofa, then sits on the chair, and finally lies down on the bed. Using two separate interaction controllers, our extended framework enables physically simulated characters to present rich interaction behaviors.